# Picosecond photoinduced-absorption studies of band-tail thermalization in hydrogenated amorphous silicon-carbon alloys

U. Eicker, A. K. Darzi, B. Wherrett, and J. I. B. Wilson
*Department of Physics, Heriot-Watt University, Riccarton, Edinburgh EH14 4AS, United Kingdom*
(Received 1 August 1988)

Band-tail thermalization of photoexcited carriers in doped and undoped $a$-$Si_{1-x}C_x$:H alloys is studied using the picosecond photoinduced-absorption technique. With carrier densities of about $10^{20}$ cm$^{-3}$ most of the charged impurity states as well as native defects are saturated and all photoinduced-absorption decays can be attributed to the band-tail width of the material. We find that carbon alloying and doping both increase the band-tail width by increasing the network disorder and by introducing new states for deeper thermalization. The optical absorption cross sections $\sigma_{\text{eff}}$ obtained for a given excitation energy decrease in high-band-gap materials and highly doped samples.

## I. INTRODUCTION

Picosecond photoinduced-absorption (PA) measurements have been widely used to study ultrafast carrier relaxation in amorphous semiconductors.[1–3] Interest has focused on hydrogenated amorphous silicon, $a$-Si:H, as an important material for optoelectronic technology and photovoltaic applications. Optimization of $p$-$i$-$n$-based amorphous silicon solar cells has included the development of a high-band-gap "window" layer using the gap-widening properties of carbon alloying.[4]

Carbon alloying influences both network disorder (band tails) and the density of midgap defect states, depending strongly on the alloying ratio. In the time domain of the excite-and-probe experiment we are able to monitor the band-tail thermalization of photoexcited carriers and hence the influence of disorder on the thermalization time.

The doping of $a$-Si:H has been successfully modelled by Street,[5] where addition of a single dopant creates pairs of ionized dopants with charged dangling bonds ($P_4^+$, $D^-$) or ($B_4^-$, $D^+$), the Fermi energy being pinned in between these band-gap energy levels. Dangling bonds (DB's) are the major defects in $a$-Si:H and its alloys. Compensation greatly reduces the DB density as the donors and acceptors now exchange electrons and do not need dangling-bond creation for the stabilizing energy reductions.

Although we assume the doping mechanism in $a$-SiC:H to be similar to that of $a$-Si:H, differences arise due to the overlapping of wider band tails with doping-related impurity levels or the altered energy location of the impurity levels with respect to the band edges. In contrast to previously published results, none of the highly doped films showed photoinduced bleaching.

Using high-energy excitation pulses we create carrier densities of about $10^{20}$ cm$^{-3}$ and saturate the doping-related charged impurity levels. We attribute all photoinduced absorption decays to the band-tail width of the material, with low-energy band-tail states having lower absorption cross sections.

In the following we present the photoinduced-absorption characteristics of a range of undoped, doped, and compensated $a$-SiC:H samples and demonstrate the effect of disorder and impurity incorporation on fast-carrier relaxation.

## II. EXPERIMENT

The samples were deposited in a capacitively coupled rf glow-discharge system using mixtures of propane and silane for the $a$-SiC:H films. Propane-based silicon carbides need lower rf input power to sustain the discharge (compared with the widely used methane mixture) and are supposed to have a low electron-spin density,[6,7] i.e., low defect density. All samples were grown with 10-W rf power applied to 100-mm-diam electrodes. Substrate temperatures were 220–250 °C and total pressure was 0.1–0.2 torr for all samples grown. Dopants were added from $B_2H_6$/Ar or $PH_3/N_2$ mixtures.

Linear transmission and absorption spectra were recorded with a Shimadzu spectrophotometer and thicknesses of the films were calculated from the interference fringes of the transmission spectra. The band gap was obtained from the usual Tauc plot. Table I gives a summary of deposition and optical parameters. The excite-and-probe method is a standard technique for investigating physical processes on the subpicosecond to nanosecond timescale. The experimental setup as shown in Fig. 1 consisted of a passively mode-locked Nd:YAG (yttrium aluminum garnet) oscillator-amplifier system where a single pulse at 1.06 $\mu$m was selected out of a train of pulses using a Pockels cell. The 530-nm wavelength used for both excite and probe beams was generated using a KDP frequency-doubling crystal. The photon energy is larger than the band-gap energy of the materials studied. The pulse duration was typically 20 psec, with excite-pulse energies varying from 4 to 16 $\mu$J. The beams were focused down to 220 $\mu$m diameter for the excite and 60 $\mu$m diameter for the probe beam to produce a homo-

 

TABLE I. Deposition and optical parameters. Absorbance $A$ is defined as $\log_{10}(I_{\text{incident}}/I_{\text{transmitted}})$, $n$ is the refractive index in the nonabsorbing region, and the volume is obtained from illuminated area and sample thickness.

| Sample | $x \equiv [C_3H_6]/[SiH_4]$<br>$y \equiv [\text{dopant}]/([C_3H_6]+[SiH_4])$ | Thickness ($\mu$m) | $E_{\text{opt}}$ (eV) | Absorbance $A$ | $\alpha$ ($\text{cm}^{-1}$) | $n$ | Volume ($10^{-8}$ $\text{cm}^3$) |
|---|---|---|---|---|---|---|---|
| A | $x=1.0$<br>$y=0$ | 0.9 | 2.25 | 0.28 | $7.16\times10^3$ | 2.3 | 3.42 |
| B | $x=0.1$<br>$y=0$ | 0.56 | 1.88 | 1.3 | $5.34\times10^4$ | 3.1 | 2.13 |
| C | $x=0.1$<br>$y=1.8\times10^{-2}$ ($B_2H_6$) | 0.745 | 1.97 | 0.79 | $2.44\times10^4$ | 2.3 | 2.83 |
| D | $x=0.1$<br>$y=10^{-2}$ ($PH_3$) | 1.15 | 1.94 | 1.02 | $2.03\times10^4$ | 2.5 | 4.39 |
| E | $x=1.0$<br>$y_1=10^{-2}$ ($B_2H_6$)<br>$y_2=10^{-2}$ ($PH_3$) | 0.4 | 2.23 | 0.2 | $1.15\times10^4$ | 2.1 | 1.52 |
| F | $x=0$<br>$y_1=2\times10^{-4}$ ($B_2H_6$)<br>$y_2=5\times10^{-4}$ ($PH_3$) | 0.26 | 1.76 | 1.51 | $1.33\times10^5$ | 3.2 | 0.99 |
| G | $x=0$<br>$y=10^{-2}$ ($PH_3$) | 0.84 | 1.77 | 2.16 | $5.92\times10^4$ | 3.2 | 3.2 |

geneously exposed area and provide good overlap and interaction of both beams. The observed incremental transmission change $\Delta T/T_0$ is proportional to a change in absorption coefficient $\alpha$ ($\Delta T/T_0 \approx \Delta\alpha/\alpha_0$). Time-dependent changes in reflectivity are not taken into consideration.

The effective cross section $\sigma$ can then be obtained from the relation

$$\Delta\alpha=(\sigma_{\text{PA}}-\sigma_{\text{PB}})N=\sigma_{\text{eff}}N\ , \tag{1}$$

where $\sigma_{\text{PA}}$ is the cross section of a photoinduced-absorption process, $\sigma_{\text{PB}}$ the cross section of a photoinduced-bleaching process, and $N$ the carrier density. With carrier densities $>10^{20}$ $\text{cm}^{-3}$ we generate a dense plasma and hence have to include the effect of Auger recombination. Using the Auger coefficient for crystalline silicon of $C=4\times10^{-31}$ $\text{cm}^6/\text{sec}$, we calculated the carrier density for $t=60$ psec as well as the Auger lifetime $\tau=1/CN^2$. Auger recombination with calculated lifetimes on the picosecond time scale should contribute to the signal decays. However, step-function behavior or slow signal recoveries on the nanosecond time scale indicate a smaller Auger coefficient $C$ for carriers thermalized into the band tails, i.e., longer Auger lifetimes $\tau$. We thus take into account only an initial Auger recombination for extended-state carriers, which reduces the plasma density.

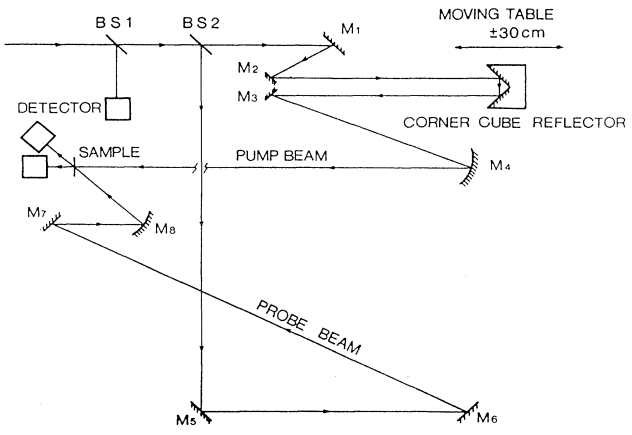


FIG. 1. Experimental arrangement for picosecond photoinduced-absorption measurements.

The radiative recombination times investigated in photoluminescence experiments peak at $10^{-5}$–$10^{-4}$ sec for $a$-Si:H and the fastest radiative lifetime observed is $\approx 8$ nsec.[8] The highest intensities used (7.5 $\text{mJ/cm}^2$) give an initial excited-carrier density of about $5\times10^{19}$ $\text{cm}^{-3}$, comparable to the intensities used in our setup. The fastest initial photoluminescence decay rate $\tau_0$ is temperature dependent and can be fitted with $\tau_0^{-1}=\nu_1+\nu_0\exp(T/T_0)$, where $\nu_1$ is the radiative rate and $\nu_0\exp(T/T_0)$ the temperature-dependent nonradiative rate. Using the obtained curve-fit parameters the nonradiative rate at room temperature with $6.3\times10^9$ $\text{sec}^{-1}$ clearly dominates the radiative rate of $10^8$ $\text{sec}^{-1}$. Increasing the carbon content shifts the average lifetime peak to shorter recombination times (up to $\approx 10^{-8}$ sec), but the quantum efficiency even measured at 77 K drops to only about 10% of the $a$-Si:H value.[9] As all our measurements are performed at room temperature, i.e., at low quantum-efficiency conditions, the nonradiative recombination should dominate any radiative band-tail recombination.

TABLE II. Experimental conditions and results from excite-and-probe measurements. (no rec. denotes no recovery.)

| Sample | $P_{input}$ ($\mu$J) | $N$ ($cm^{-3}$) without Auger recombination | $\Delta T/T_0$ | $\Delta\alpha$ ($cm^{-1}$) | $\tau_{Auger}$ (psec) | $N$ ($cm^{-3}$) including Auger recombination | $\sigma_{eff}$ ($cm^2$) | $\tau_{1/2}$ (nsec) |
|---|---|---|---|---|---|---|---|---|
| A | 6 | $1.3\times10^{20}$ | 0.18 | $1.3\times10^{3}$ | 150 | $9.5\times10^{19}$ | $1.3\times10^{-17}$ | 3.7 |
| B | 9 | $9.2\times10^{20}$ | 0.56 | $2.9\times10^{4}$ | 3 | $1.4\times10^{20}$ | $2\times10^{-16}$ | no rec. |
| C | 9 | $6.4\times10^{20}$ | 0.27 | $6.6\times10^{3}$ | 6 | $1.4\times10^{20}$ | $4.6\times10^{-17}$ | 5.5 |
| D | 4 | $1.2\times10^{20}$ | 0.2 | $4.1\times10^{3}$ | 165 | $9.3\times10^{19}$ | $4.3\times10^{-17}$ | no rec. |
| E | 16 | $8\times10^{20}$ | 0.07 | $7.8\times10^{2}$ | 4 | $1.4\times10^{20}$ | $5.5\times10^{-18}$ | 0.95 |
| F | 9 | $2\times10^{21}$ | 0.67 | $8.9\times10^{4}$ | 0.7 | $1.4\times10^{20}$ | $6.2\times10^{-16}$ | no rec. |
| G | 6 | $4\times10^{20}$ | 0.3 | $2.1\times10^{4}$ | 17 | $1.3\times10^{20}$ | $1.5\times10^{-16}$ | no rec. |

## III. RESULTS

The main experimental parameters and results are listed in Table II. Photoinduced absorption decays were measured in two undoped SiC:H samples with $[C_3H_8]/[SiH_4]$ ratios of $x=1.0$ and 0.1, respectively. The induced absorption was instantaneous within the pulse width for both samples. Before the onset of final-state saturation the magnitude of the incremental change, $\Delta T/T$, could be increased using higher laser-input energy: higher population densities of photoexcited carriers increase the free-carrier absorption and therefore the transmission drop $\Delta T$. Varying the input energy from 6 to 14 $\mu$J (sample A) changes the incremental transmission $\Delta T/T_0$ from 0.18 to 0.25, thus giving similar effective absorption cross sections $\sigma_{eff}$ ($1.3\times10^{-17}<\sigma_{eff}<1.38\times10^{-17}$ $cm^2\approx\Delta T/N$). For $x=0.1$ the PA characteristic showed behavior similar to a typical low-defect-density $a$-Si:H film[10] with no recovery in the monitored time range of 1.4 nsec. As none of the samples recovered to the initial transmission level within the timing period possible with this experimental arrangement, we introduced a recovery time $\tau_r$ for the half maximum value of transmission $T_{1/2}$. The sample with $x=1.0$ gradually recovered with $\tau_r=3.7$ nsec (see Fig. 2).

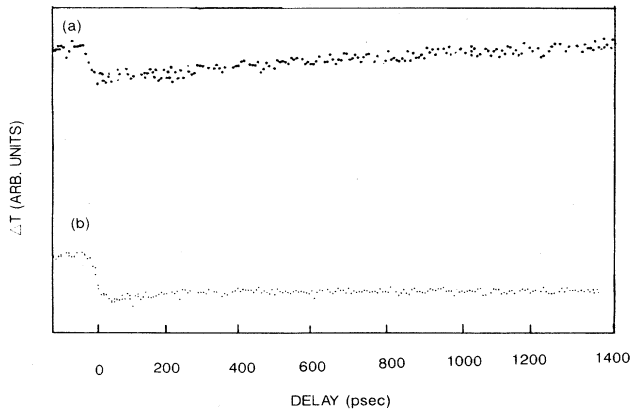


FIG. 2. Photoinduced absorption $\Delta\alpha(t)=-\Delta T(t)$ in undoped $a$-SiC:H. (a) Sample A [$(C_3H_8)$:$(SiH_4)=1$]; (b) sample B [$(C_3H_8)$:$(SiH_4)=0.1$].

The compensated $a$-$Si_{0.5}C_{0.5}$:H sample with a high compensation ratio [both dopants with $y=10^{-2}$ (see Table I)] was compared with an $a$-Si:H sample having a compensation ratio of $2\times10^{-4}$ ($B_2H_6$) and $5\times10^{-4}$ ($PH_3$). Again the low compensated $a$-Si:H film showed no recovery in the time scale, and in agreement with measurements by Jackson *et al.*[2] The highly compensated $a$-SiC:H film with $x=1.0$ had $\tau_r=0.95$ nsec, but in contrast with Jackson's results for $a$-Si:H it did not go over to an induced transmission region (see Fig. 4).

Figure 3 shows results for the boron-doped sample ($x=0.1$) with $\tau_r=5.5$ nsec as well as the phosphorus-doped $a$-SiC:H and $a$-Si:H samples, both of which did not show any recovery.

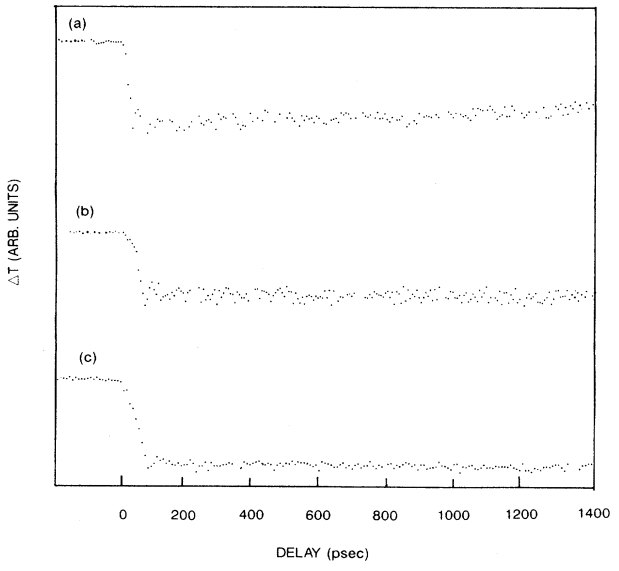


FIG. 3. Photoinduced absorption in doped $a$-SiC:H and $a$-Si:H. (a) Sample C ($[C_3H_8]$:$[SiH_4]=0.1$, $[B_2H_6]/([C_3H_8]+[SiH_4])=1.8\times10^{-2}$); (b) sample D ($[C_3H_8]$:$[SiH_4]=0.1$, $[PH_3]/([C_3H_8]+[SiH_4])=10^{-2}$); (c) sample G ($[C_3H_8]$:$[SiH_4]=0$, $[PH_3]/[SiH_4]=10^{-2}$).

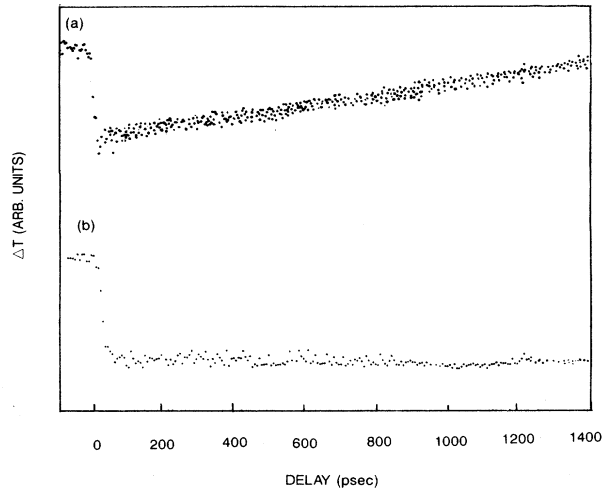


FIG. 4. Photoinduced absorption in compensated $a$-SiC:H and $a$-Si:H. (a) Sample E ($[C_3H_8]:[SiH_4]=1$, $[B_2H_6]/([C_3H_8]+[SiH_4])=10^{-2}$, $[PH_3]/([C_3H_8]+[SiH_4])=10^{-2}$); (b) sample F ($[C_3H_8]:[SiH_4]=0$, $[B_2H_6]/[SiH_4]=2\times10^{-4}$, $[PH_3]/[SiH_4]=5\times10^{-4}$).

## IV. DISCUSSION

The absorption process in amorphous semiconductors consists of both band-to-band and intraband absorption:

$$\alpha=\alpha_{vc}(f_e,f_h)+\alpha_{\text{intra}}(N)\ , \tag{2}$$

where $f_e$ ($f_h$) is the occupation probability of the final (initial) state. With a probe-beam energy greater than the band gap the valence- to- conduction-band transitions remain unchanged since there is no saturation at the irradiance used, so it is intraband absorption of the photoexcited carriers which results in the observed photoinduced absorption.

Various models have been proposed to interpret the subsequent PA recoveries and possible bleaching effects. It is generally agreed that directly after the excitation carriers relax into the band tails. Recently this initial band-tail thermalization process has been separated into a direct hopping and a multiple trapping regime, where only the latter is temperature dependent.[3,11,12] The segregation time $\tau_s=\nu_0^{-1}\exp(3T_w/T)$ ($\nu_0$ is the fastest hopping frequency, $T_w$ the band-tail width in K) between these two regimes can be used to deconvolute electron and hole thermalization, as the band-tail widths of valence and conduction bands differ and thus give different $\tau_s$. In $a$-Si:H, band-tail widths of 600 K for the valence band and 300 K for the conduction band give $\tau_s=4$ psec for electrons and $\tau_s=80$ psec for holes; therefore fast temperature-dependent decays $<80$ psec, i.e., multiple trapping of electrons, can be attributed to electron thermalization. As the band tail is widened with carbon alloying [$T_w>T_w(a\text{-Si:H})$], the direct hopping regime is extended for both carriers, and deconvolution is no longer possible. Furthermore, no fast decays ($<100$ psec) have been observed in our samples, even using highly-$PH_3$-doped samples.

The subsequent recovery of the PA has been interpreted by a deep-trapping model[13] or a pure band-tail thermalization process[2] which includes thermalization into donor and acceptor levels in the case of doped samples. W. B. Jackson performed PA measurements on samples with varying defect densities. Increasing dangling-bond densities did not lead to faster PA decays; hence changes in the optical-absorption cross sections in the band tails are the suggested cause of the signal decay. Our results in $a$-SiC:H can be explained by band-tail thermalization as the dominant process, the band-tail width being the characteristic parameter for the signal recovery. Trapping in doping-related impurity levels in the band tails, with different absorption cross sections, proves to be of less influence on the signal decay. Contrary to previously published results, we do not observe a photoinduced bleaching either for the highly doped $a$-SiC:H or $a$-Si:H samples. The reported photoinduced bleaching in highly doped $a$-Si:H films was obtained using low-energy densities of 0.1–0.2 nJ (Ref. 3) and 8 nJ (Ref. 2), respectively. The effect is attributed to electron capture by $P_4^+$ states which subsequently block transitions from the valence band into these charged impurity states (CIP's). However, using high excitation energies of 4–16 $\mu$J, we generate high carrier concentrations such that intraband-induced absorption dominates the transmission on the time scale of the experiments and no photoinduced bleaching can be observed.

A short description of the effect of carbon alloying is necessary here.

Sub-band-gap absorption spectra of $a$-SiC:H show similar band-tail characteristics as $a$-Si:H up to a carbon content of about 40%. Accordingly, the low carbon content PA characteristic is similar to a typical $a$-Si:H sample. The analysis of the dielectric-constant spectra leads to a model where Si—Si bonds determine the structure up to a considerable carbon content. The carbon is mainly incorporated as $CH_3$ and $CH_2$ groups. For $x>0.4$ the Si-based lattice destabilizes and Si—C bonds as well as polymeric $a$-$(CH)_m$ form a more polymerlike lattice.[14] These structural changes for high-carbon-content alloying increase both band-tail width and band-gap energy considerably.[15]

Photoexcited carriers can thus thermalize further into the band gap. Assuming lower absorption cross sections for more localized deeper energy states, this band-tail thermalization leads to a slow recovery of the initial free-carrier-induced absorption (nanosecond time scale). This effect of thermalization into wider band tails is confirmed by comparing a high- ($x=1.0$) and low- ($x=0.1$) carbon-content sample: the high-carbon-content sample shows a signal recovery with $\tau_r=3.7$ nsec, whereas in the low-carbon-content film with sharper exponential tails no signal recovery is observed (see Fig. 2). Further thermalization is prevented until the onset of deep trapping or recombination, which does not occur in the time scale used for these experiments. Recombination times as measured by the transient photocurrent method depend strongly on sample preparation, doping, and temperature, but are always longer than $10^{-7}$ sec.[16]

Single doping of *a*-Si:H introduces narrow donor or acceptor levels in the band tails which should exceed the band-tail density when the doping ratio is higher than $\approx 10^{-4}$. Sub-band-gap absorption spectra in boron-doped *a*-SiC:H show an increase both in Urbach energy (e.g., network disorder) and defect density with increased boron doping.[15] We attribute the slow decay of the singly-boron-doped *a*-SiC:H film (sample C), as shown in Fig. 3 with $\tau_r = 5.5$ nsec, to the increase of disorder (wider band tails) rather than to the different absorption cross sections of the doping-related impurities; the decay is faster than for the undoped film of the same carbon ratio (no recovery), but slower than for the highly alloyed film ($\tau_r = 3.7$ nsec).

No similar sub-band-gap spectra have been published for phosphorus-doped *a*-SiC:H. The singly-phosphorus-doped *a*-SiC:H film did not show a signal recovery, contrasting the result for the boron-doped sample. In most semiconductors, valence-band intraband absorption cross sections are larger than corresponding conduction-band cross sections. Furthermore, valence-band tails in amorphous semiconductors are broader than conduction-band tails. Hence further thermalization and hole-dominated intraband absorption contribute to the signal decay in the boron-doped sample.

To confirm the exclusion of the deep trapping-recombination model we studied the influence of dangling-bond reduction through compensated doping. If the signal decay is due to deep trapping, the reduction of midgap states should increase the decay time. Compensation introduces donors and acceptors superimposed on the band tails without having to form the compensating dangling bonds required by single doping in these materials. Low compensation ratios ($10^{-4}$) as shown for sample F (Fig. 4) introduce doping-related impurities in the *a*-Si:H film. However, the PA process is not affected by these additional impurities and the signal does not recover in the nanosecond time scale. The highly alloyed *a*-SiC:H sample with a compensation ratio of $10^{-2}$ has a recovery time of $\tau_r = 0.95$ nsec, i.e., it recovers faster than the undoped *a*-SiC:H sample of equal carbon ratio; therefore, recombination via midgap states can be excluded. Compensated films are known to have additional states above the valence band due to boron-phosphorus complexes which allow holes to thermalize further into the band gap,[17] thus contributing to the faster signal decay.

The magnitude of incremental transmission $\Delta T/T$ and hence the initial absorption cross section $\sigma$ depend on the band gap and absorption coefficient of the material: using pump energies ($E_{\text{pump}}$) of 2.33 eV in wide-band-gap materials, carriers are excited to states close to the conduction-band edge ($E_{\text{opt}} \approx 2.25$ eV), which are strongly localized and have lower absorption cross sections. Equally, no induced absorption could be observed in a phosphorus-doped highly-carbon-alloyed sample with $E_{\text{opt}} = 2.65$ eV $> E_{\text{pump}}$. Figure 5 shows the relation between the optical band-gap and absorption cross section $\sigma$: the trend of increasing $\sigma$ with decreasing optical band gap is clearly visible. Furthermore, undoped or slightly doped materials have higher cross sections than highly doped materials of comparable optical band gap.

To further investigate fast-carrier relaxation, we performed picosecond transient grating experiments on some of the samples. This allows us to distinguish directly between extended and localized states. The results confirm the assumption of fast-carrier relaxation from extended to localized states ($\approx 20$ psec) for low-carbon-content

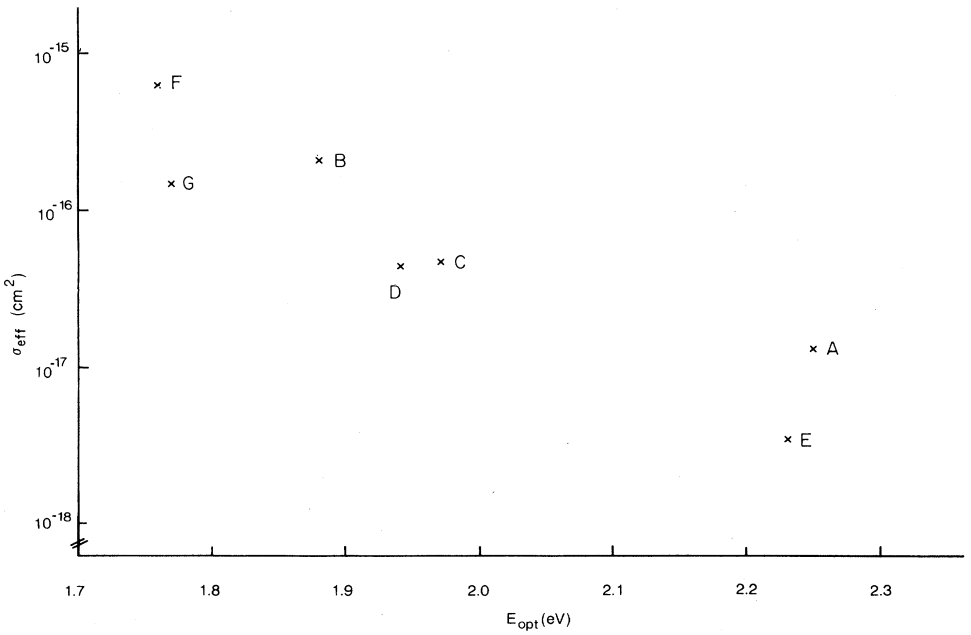


FIG. 5. Optical cross section $\sigma_{\text{eff}}$ vs optical band gap $E_{\text{opt}}$. High band gaps and high doping ratios decrease the magnitude of the initial intraband absorption cross section.

samples with no subsequent decay in the picosecond time scale. A detailed analysis of the transient grating as well as two-beam phase-conjugation experiments will be published later.

## V. CONCLUSIONS

In conclusion, PA characteristics in *a*-SiC:H alloys are shown to depend strongly on the disorder of the amorphous network and thus on the band-tail width of the material. Both single and compensated doping contribute to the increase in network disorder and new states for deeper thermalization are introduced by compensated doping (boron-phosphorus complexes). Band-tail states with lower energy are shown to have lower absorption cross sections, leading to a decay of photoinduced absorption. Finally, saturation of charged impurity states and dominance of intraband absorption have been obtained using high excitation energies. All PA decays can thus be attributed to the band-tail width, i.e., the disorder of the material. The optical-absorption cross section $\sigma_{\text{eff}}$ for a given excitation energy decreases in high-band-gap materials and highly doped samples.

## ACKNOWLEDGMENTS

We thank J. Tauc for very helpful comments on our results. We also thank A. Qayyum and S. K. Al Sabbagh for providing some of the samples used in this work and Yuk Tak Chow for his assistance with the laser system. The work of U. Eicker was partially supported by Heriot-Watt University and A. Darzi acknowledges support from the Iraqi Government.

[1]O. E. Ackley and J. Tauc, Phys. Rev. Lett. **43**, 715 (1979).
[2]W. B. Jackson, C. Doland, and C. C. Tsai, Phys. Rev. B **34**, 3023 (1986).
[3]Z. Vardeny, C. Thomsen, and J. Tauc, Solid State Commun. **65**, 607 (1988).
[4]Y. Tawada, K. Tsuge, M. Kondo, H. Okamoto, and Y. Hamakawa, J. Appl. Phys. **53**, 5273 (1982).
[5]R. A. Street, Phys. Rev. Lett. **49**, 1187 (1982).
[6]S. Nitta, A. Hatano, M. Yamada, M. Ohsawa, and S. Ishida, J. Non-Cryst. Solids **59-60**, 557 (1983).
[7]A. Qayyum, J. I. B. Wilson, K. Ibrahim, and S. K. Al-Sabbagh, in *Proceedings of the European Materials Research Society, Symposium C, Strasbourg, 1987,* edited by P. Koidl and P. Oelhafen (Les Editions de Physique, Paris, 1987), Vol. XVII, p. 463.
[8]B. A. Wilson, P. Hu, J. P. Harbison, and T. M. Jedju, Phys. Rev. Lett. **50**, 1490 (1983).
[9]W. Siebert, K. Jahn, and W. Fuchs, J. Non-Cryst. Solids **77&78**, 869 (1985).
[10]G. Noll and E. O. Gobel, J. Non-Cryst. Solids **92-98**, 147 (1987).
[11]Z. Vardeny, J. Strait, O. Pfost, J. Tauc, and B. Abeles, Phys. Rev. Lett. **48**, 1332 (1982).
[12]O. Monroe, Phys. Rev. Lett. **54**, 146 (1985).
[13]J. Strait, Ph.D. thesis, Brown University, Providence, Rhode Island, 1984.
[14]J. Sotiropoulos and G. Weiser, J. Non-Cryst. Solids **97-98**, 1087 (1987).
[15]A. Asano and T. Ichimura, Jpn. J. Appl. Phys. **25**, L388 (1986).
[16]H. Oheda, Philos. Mag. B **52**, 857 (1985).
[17]R. A. Street, O. K. Biegelsen, and J. C. Knights, Phys. Rev. B **24**, 969 (1981).